JOURNAL OF MATERIALS SCIENCE 27 (1992) 77–82

Formation and thermal decomposition of rare-earth carbonates

K. FOGER, M. HOANG, T. W. TURNEY*
CSIRO Division of Materials Science and Technology, Locked Bag 33, Clayton, Victoria, Australia 3168

The preparation of carbonate-containing rare-earth compounds and their thermal decomposition in 0%–17% CO_2/N_2 gas streams has been studied. Three types of rare-earth carbonate or hydroxycarbonate were produced by precipitation; with ammonium bicarbonate as the precipitant, $La_2(CO_3)_3$,$CeOCO_3$ and $Ln(OH)_x(CO_3)_y$ (Sm, Tb, and Yb) were obtained, whereas with Na_2CO_3, only the normal carbonate, $Ln_2(CO_3)_3$ (La, Sm, Tb, Er and Yb) was found. Temperature programmed decomposition studies revealed that the normal carbonate decomposed stepwise via a dioxocarbonate, $Ln_2O_2CO_3$, to the oxide. In contrast, the hydroxycarbonates decomposed directly to the oxide. The presence of CO_2 during heating had minimal effect on the decomposition of $Ln_2(CO_3)_3$ to $La_2O_2CO_3$ but raised significantly the decomposition temperature of $Ln_2O_2CO_3$ to the oxide. As CO_2 is a major product of the rare-earth oxide catalysed oxidative coupling of methane, these observations indicate that the state of catalyst carbonation will be dependent on the reaction temperature, overall catalyst selectivity and preparative method.

1. Introduction

There is considerable current interest in the use of rare-earth oxides as components in catalysts for the oxidative coupling of methane to C_{2+} hydrocarbons, performed typically at temperatures of 600–900 °C [1, 2]. Establishing the constitution of the working catalyst is of crucial importance in understanding the nature of this reaction and hence improving C_2 yields (which are generally below 20%). As carbon dioxide is one of the unwanted, but ubiquitous, products of the partial oxidation of methane, identification of the stability ranges of various rare-earth carbonates, especially in dilute CO_2 streams is essential.

The synthesis of rare-earth carbonates has been the subject of numerous investigations [3–9]. They have revealed that under appropriate preparative conditions, variable amounts of hydroxide ligand may be incorporated. Thus, hydrothermal ageing of precipitates, obtained from reaction of bicarbonate with solutions containing rare-earth salts, produced $Ln(OH)CO_3$ (Ln = La, Nd, Sm) [4]. The pure carbonate phase, $Ln_2(CO_3)_3 \cdot nH_2O$ (Ln = Y, Er, Ho, Gd, Nd and Sm), has been obtained by hydrolysis of rare-earth trichloroacetate [5]. However, on precipitation from rare-earth chloride solutions with $NH_4CCl_3CO_2$, other workers have reported the formation of either normal carbonates ($Ln_2(CO_3)_3 \cdot nH_2O$, Ln = La, Nd, Sm, Eu, Gd, Tb, Dy or Ho) or basic carbonates of the type, $Ln(OH)_x(CO_3)_y \cdot nH_2O$ (Ln = Ce, Pr, Er, Tm, Yb or Lu) [6]. It has been suggested that the normal carbonates hydrolyse during synthesis, resulting in the formation of basic carbonates, with hydrolysis occurring more rapidly with the less basic (i.e. heavier) lanthanides [7]. Slow hydrolysis of urea in hot dilute acid solutions of Pr, Nd, Sm, Eu, Gd, Tb and Dy, has also been reported to afford mixtures of $Ln(OH)_x(CO_3)_y$ and $Ln_2(CO_3)_3 \cdot nH_2O$ [8].

Previous studies of various rare-earth carbonates have demonstrated that thermal decomposition is quite sensitive to starting composition [7, 10–13]. It has also been shown that the normal carbonates decompose via intermediate dioxocarbonates [10, 12]. However, there are discrepancies between decomposition temperatures, as determined by thermogravimetric analysis (TGA), by different workers. These have been variously attributed to differences in particle size, heating conditions, or difficulties in preparing pure and uniform products [7, 8].

In this study, temperature programmed decomposition (TPD), measuring only evolved CO_2, and thermogravimetric analysis (TGA), measuring the sum of H_2O and CO_2 mass losses, were each employed to investigate thermal decomposition of the various rare-earth carbonate species. Furthermore, effects of CO_2 partial pressure on decomposition temperatures were studied.

2. Experimental procedure

2.1. Materials

Nitrate salts of the trivalent rare-earths were prepared from the oxides by the method given by Marsh [14].

---

* Author to whom all correspondence should be addressed.

0022–2461/92 $03.00 + .12

Ammonium "carbonate" comprising a mixture of ammonium bicarbonate and ammonium carbamate (ratio of 5:1) and $(NH_4)_2[Ce(NO_3)_6]$ (99%) were supplied by Ajax Chemicals, Australia.

2.2. Preparation of rare-earth carbonates

Typically, $Ln(OH)_x(CO_3)_y$ were prepared by addition of an aqueous solution of NH_4HCO_3 (24 g in 1 litre) dropwise to a stirred solution of the metal nitrate (3 litre, 0.016 M), while a stream of CO_2 was bubbled through the solution. The resultant hydrogel was separated by centrifugation, washed first with distilled water (4 litre) to a final conductivity of $< 2.5\ \text{m s}^{-1}$ and then with acetone (1.5 litre). Products were dried initially at room temperature in a nitrogen stream, then *in vacuo* for 10–30 h and finally at 110 °C for 16 h. The compounds, $Ln_2(CO_3)_3$, were prepared as above but by substituting Na_2CO_3 for ammonium bicarbonate. $Sm(OH)CO_3$ was prepared according to Christensen [4], using $KHCO_3$ as precipitant, followed by hydrothermal treatment in an unstirred autoclave (Parr model 4740, 316SS) at 300 °C for 30 h.

2.3. Characterization

Details of the temperature programmed decomposition apparatus are shown in Fig. 1. The reactor consisted of a 6 mm o.d. silica tube, with a silica frit in the centre, surrounded by a temperature programmable furnace. Temperatures were measured by a type-K thermocouple embedded in the sample. In a typical run, the sample (30 mg, 60–80 mesh) was placed in the reactor and pretreated with N_2 or He (20 ml min^{-1}) at 110 °C (or 50 °C for Ce carbonate). Then the reactor was cooled down to the starting temperature of TPD run (usually 30–40 °C) and He or CO_2/He carrier gas (20 ml min^{-1}) was passed over the sample while the temperature was programmed linearly to 1000 °C at a rate of 20 °C min^{-1}. Water was removed by use of a trap cooled to between -15 and -20 °C with a mixture of dry ice and ethane-1,2-diol. The gas stream was mixed and controlled by flow controllers and micrometering valves and analysed with a thermal conductivity detector.

Thermogravimetric analysis was carried out using a Stanton-Redcroft STA-700, simultaneous thermal analyser (N_2 atmosphere, ramp rate = 10 °C min^{-1}). Infrared spectra were recorded with a Mattson Cygnus 100 FTIR as KBr discs. X-ray diffraction traces were obtained using a Siemens D500 (CuK_α radiation, step scan size = 0.04°). TEM was performed with a Jeol 100 CX electron microscope on samples ultrasonically dispersed in hexane and collected on a holey carbon grid.

3. Results and discussion

3.1. Formation of rare-earth carbonates

Solutions of lanthanum nitrate afforded a crystalline phase by treatment with either ammonium or sodium carbonate solution. The powder XRD pattern of the material (*d*-spacings (relative intensities) = 0.480(10), 0.432(3), 0.322(4), 0.263(2) nm) was different from that reported for $La_2(CO_3)_3 \cdot 8H_2O$ (JCPDS 25-1400). The product was identified as anhydrous $La_2(CO_3)_3$ from decomposition data (TGA and TPD). On addition of either Na or NH_4 carbonate, $[Ce(NO_3)_6]^{2-}$ solutions precipitated a yellow, X-ray amorphous material, whose thermal analysis best fitted the composition $CeOCO_3$.

With samarium nitrate solutions, precipitation with sodium carbonate afforded a crystalline phase, with an XRD powder pattern identical to that reported for $Sm_2(CO_3)_3 \cdot 2.85H_2O$ [15]. In contrast, ammonium bicarbonate precipitated an X-ray amorphous material, consisting of homogeneous 10–20 nm sized flakes (Fig. 2a). A comparison of the infrared spectra of crystalline and amorphous samarium carbonate phases, revealed some difference in the OH^- stretching region; the amorphous material showed a sharp peak at 3420 cm^{-1} superimposed on a broad water peak, whereas only the broad water peak was evident in the normal carbonate.

Samarium hydroxycarbonate, prepared by hydrothermal treatment at 300 °C of the precipitate from $Sm(NO_3)_3$ solution and $KHCO_3$, was highly crystalline, with an XRD powder pattern which indicated the formation of the known phase, $Sm(OH)CO_3$ (JCPDS 26-948) [4]. Examination of $Sm(OH)CO_3$ by TEM revealed irregular 5 µm aggregates composed of 200 nm crystallites (Fig. 2b). In contrast to the amorphous samarium hydroxycarbonate phase, its

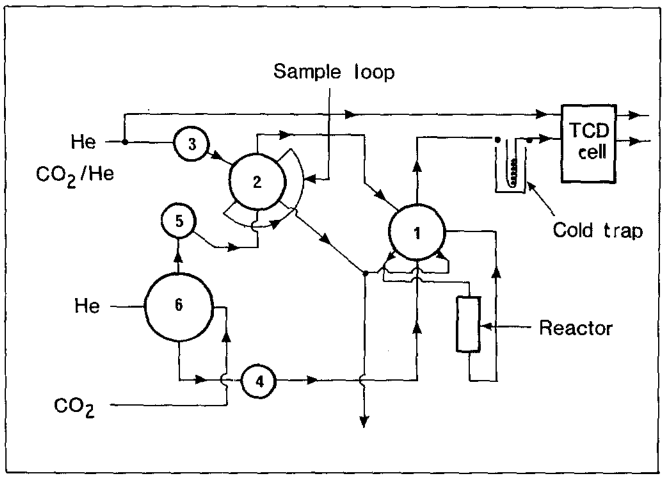

Figure 1 Temperature programmed decomposition apparatus.

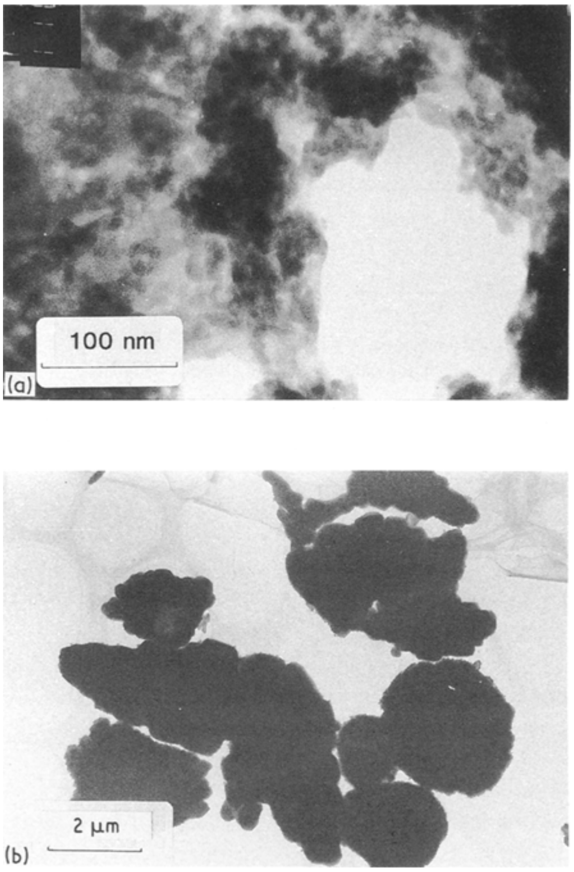

Figure 2 Transmission electron micrographs of (a) $Sm(OH)_x(CO_3)_y$ and (b) $Sm(OH)CO_3$.

infrared spectrum is characterized by two sharp OH bands at 3630 and 3470 cm^{-1}.

In a manner similar to Sm, both Tb and Yb formed normal carbonates, $Ln_2(CO_3)_3$, with sodium carbonate and amorphous hydroxycarbonates, $Ln(OH)_x(CO_3)_y$, with ammonium bicarbonate as precipitant.

3.2. Thermal decomposition

Thermogravimetric analysis (TGA), which measured the sum of CO_2 and H_2O weight losses, showed three different decomposition modes for the various carbonate species produced from ammonium carbonate (Fig. 3).

(i) $La_2(CO_3)_3$ decomposed to the oxide in two distinct steps via $La_2O_2CO_3$.

(ii) Ce "carbonate" exhibited a single decomposition step to the oxide with a weight loss of 19%, corresponding to a starting composition of $CeOCO_3$.

(iii) Samarium hydroxycarbonate of the type $Sm(OH)_x(CO_3)_y$, decomposed between 200 and 600 °C in a single step.

Analytical data obtained by TPD and TGA from carbonates of La, Sm, Tb, Er, Yb and Ce, prepared using ammonium bicarbonate as precipitant, are summarized in Table I. The TPD data for the $La_2(CO_3)_3$ phase corresponded well with the TGA profile (Fig. 4). The two peaks observed at 480 and 750 °C, indicated a two-step decomposition of $La_2(CO_3)_3$, via the dioxocarbonate, $La_2O_2(CO_3)$, to the oxide, La_2O_3. Weight losses for the two stages (Table I), as determined by TGA and calculated by TPD were similar and in good agreement with the values expected (19.2% and 9.6%, respectively) for the decomposition,

$$La_2(CO_3)_3 \xrightarrow{2CO_2} La_2O_2CO_3 \xrightarrow{CO_2} La_2O_3$$

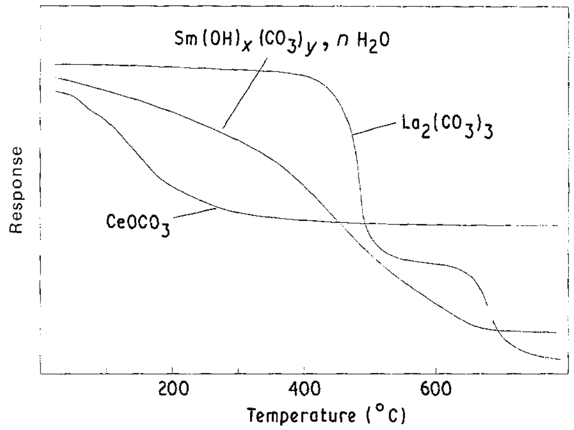

Figure 3 Thermogravimetric analysis (TGA) of $La_2(CO_3)_3$ $Sm(OH)_x(CO_3)_y \cdot nH_2O$ and $CeOCO_3$.

TABLE I Thermal analytical data for rare-earth carbonates from ammonium bicarbonate

	% weight loss				Species[b] present
	First step		Second step		
	TGA	TPD[a]	TGA	TPD[a]	
La	18.6	19.0	8.6	9.5	$La_2(CO_3)_3$
Sm	21.4	17.6	2.4	3.0	33% $Sm_2(CO_3)_3$ 67% $Sm(OH)_{1.77}(CO_3)_{0.60}$
Tb	20.7	18.7	2.9	3.2	36% $Tb_2(CO_3)_3$ 64% $Tb(OH)_{1.77}(CO_3)_{0.61}$
Er	16.2	13.1	2.5	3.2	37% $Er_2(CO_3)_3$ 63% $Er(OH)_{2.14}(CO_3)_{0.43}$
Yb	18.4	15.1	1.9	2.0	24% $Yb_2(CO_3)_3$ 76% $Yb(OH)_{1.74}(CO_3)_{0.63}$
Ce	19.0	19.6	–	–	$CeOCO_3$

[a] Based on CO_2 evolved.

[b] Calculated from TPD data, ignoring the water content of each sample.

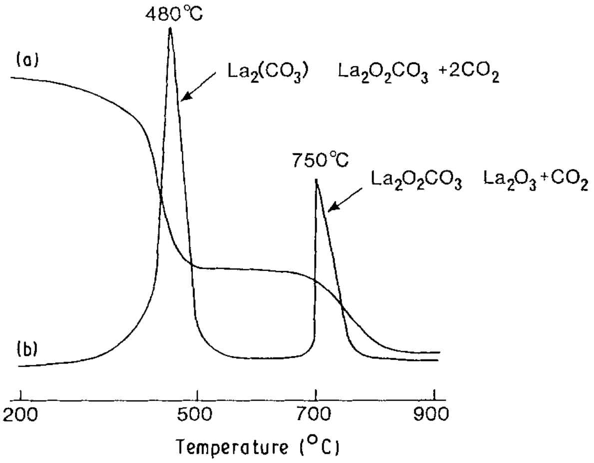

Figure 4 (a) TGA and (b) TPD of $La_2(CO_3)_3$.

TABLE II Temperature programmed decomposition data of rare-earth carbonate derived from Na_2CO_3

Element	% weight loss[a]				Degree of hydration
	TPD		Theoretical[b]		
	Step 1	Step 2	Step 1	Step 2	
Sm	16.7	8.1	18.3	9.1	$Sm_2(CO_3)_3 \cdot 2.6H_2O$
Tb	16.0	7.9	17.6	8.8	$Tb_2(CO_3)_3 \cdot 3.0H_2O$
Yb	15.1	7.5	16.7	8.4	$Yb_2(CO_3)_3 \cdot 3.2H_2O$

[a] Based on CO_2 evolved.

[b] Calculated for anhydrous $Sm_2(CO_3)_3$, $Tb_2(CO_3)_3$ and $Yb_2(CO_3)_3$. The difference from the observed values arises from the contribution of water to the formula weight in the calculations, which are based on the assumption that the carbonates are anhydrous.

Because TPD only monitors CO_2 liberation and not H_2O loss, this result indicated that, under the preparative conditions employed here, the $La_2(CO_3)_3$ sample was not hydrated. As with $La_2(CO_3)_3$, results obtained on $CeOCO_3$ from TGA and TPD were in good agreement, again pointing to the formation of an anhydrous carbonate.

The normal carbonates of Sm, Tb and Yb, precipitated with Na_2CO_3, exhibited significantly different thermal behaviour (Table II) to the hydroxycarbonates, prepared from NH_4HCO_3. The TPD trace of samarium carbonate, $Sm_2(CO_3)_3 \cdot 2.85H_2O$, (Fig. 5) is similar to that of $La_2(CO_3)_3$ with two decomposition steps, having an evolved CO_2 ratio of 2:1. Similar profiles were obtained for Tb and Yb carbonates and thermal analytical data are shown in Table II.

The temperatures at which the dioxocarbonates, $Ln_2O_2CO_3$, decompose have been reported to decrease with increasing Ln atomic number [10]. This trend was observed for the four carbonates studied here, with the temperature required to decompose $La_2O_2CO_3$ to La_2O_3 being 750 °C, but only 540 °C for $Yb_2O_2CO_3$ (Fig. 6). A less pronounced dependence on the nature of the rare-earth was observed for the first stage of the decomposition [$Ln_2(CO_3)_3$ to $Ln_2O_2CO_3$].

TPD data for the hydroxycarbonates, $Ln(OH)_x(CO_3)_y \cdot nH_2O$, showed very broad peaks with maxima around 350–450 °C and small sharp peaks at higher temperatures; TPD and TGA traces are shown for $Sm(OH)_x(CO_3)_y \cdot nH_2O$ in Fig. 7. On heating, the hydroxycarbonates liberated their water during the initial stages of decomposition, with the weight loss for the first step as measured by TGA (CO_2 and H_2O) being higher than that determined from TPD (CO_2 only) experiments. However, formation of CO_2 in the second step, which is attributed to the decomposition of $Ln_2O_2CO_3$ to the Ln_2O_3, was almost identical to that found by TPD. Table I shows the weight loss in the second step decomposition of Sm, Tb, Er and Yb hydroxycarbonates, to be much less than that expected on the basis of a pure intermediate $Ln_2O_2CO_3$ phase. Instead, it appears that 25%–37% Ln_2O_3 was derived from $Ln_2O_2CO_3$ while the remainder was formed directly from the hydroxycarbonate in the first step. Thus precipitation with ammonium carbonate yields, not a single pure hydroxycarbonate phase, but a mixture of hydroxycarbonate and normal carbonate. The compositions of carbonate precursors were calculated from TPD data and are listed in Table I. In that situation, $Ln(OH)_x(CO_3)_y$ decomposed directly to the oxide while the minor amount of $Ln_2(CO_3)_3$ decomposed via a dioxocarbonate, resulting in the appearance of a small high-temperature decomposition peak. This observation contradicts published data by Alkinc and Sordelet [13] who claimed that $Ln(OH)_x(CO_3)_y$ decomposes via $Ln_2O_2CO_3$ as an

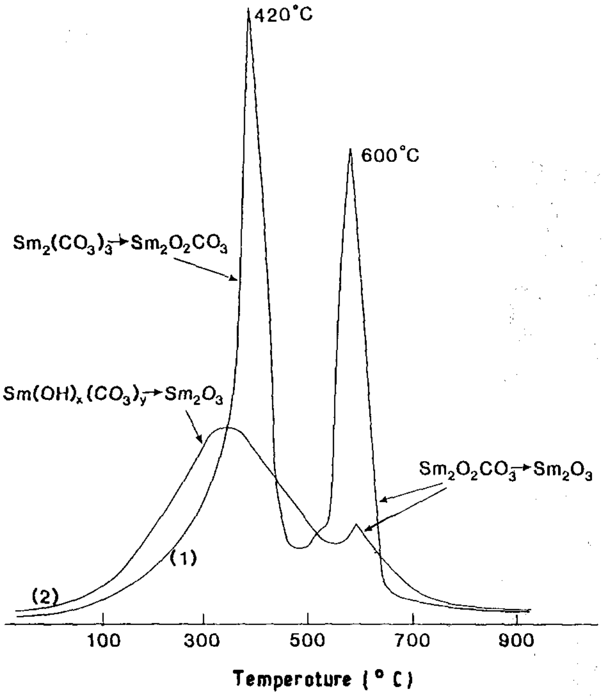

Figure 5 Temperature programmed decomposition of (a) $Sm_2(CO_3)_3$ and (b) $Sm(OH)_x(CO_3)_y$.

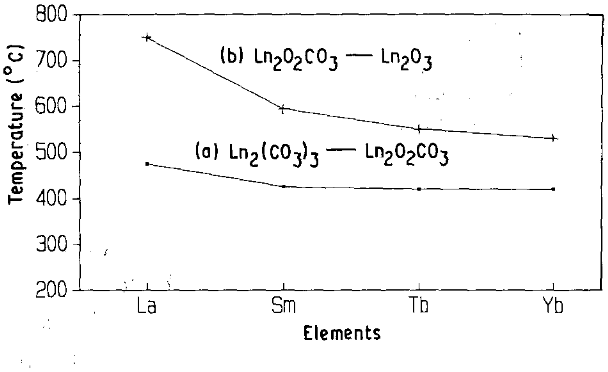

Figure 6 Decomposition temperatures of rare-earth carbonates as measured by TPD.

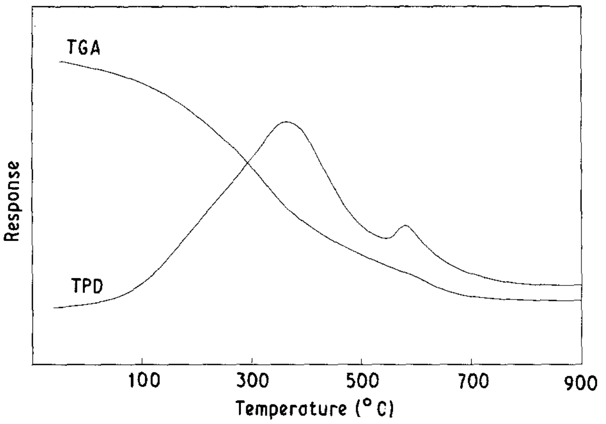

Figure 7 TPD and TGA of $Sm(OH)_x(CO_3)_y \cdot nH_2O$.

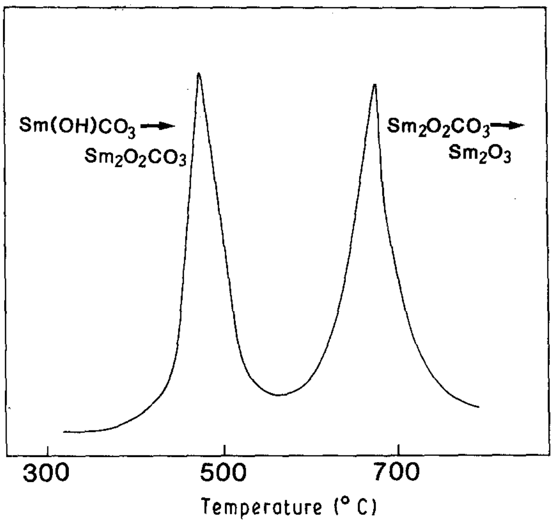

Figure 8 TPD of $Sm(OH)CO_3$.

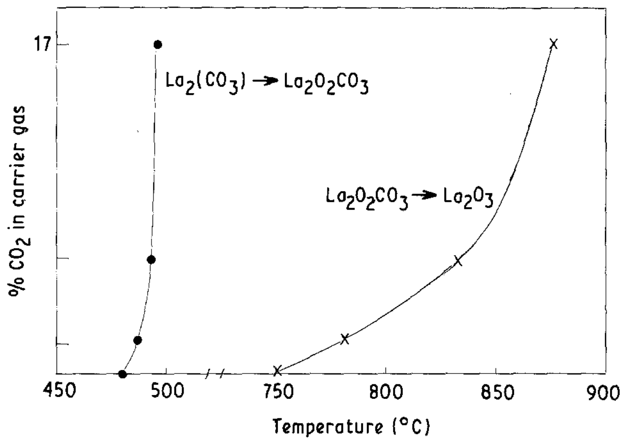

Figure 9 Effect of CO_2 on thermal decomposition of $La_2(CO_3)_3$.

intermediate. Possibly, such discrepancies arise from the different particle size of carbonates used in the two studies. TEM of the carbonates in this study showed a narrow particle size distribution in the range 10–20 nm, while carbonates studied by Alkinc and Sordelet consisted of 10 μm particles. The importance of particle size on mode of decomposition is demonstrated with $Sm(OH)CO_3$ prepared by hydrothermal treatment (particle size about 5 μm), which exhibited significantly different thermal behaviour to the hydroxycarbonate prepared from NH_4HCO_3. The TPD profile of $Sm(OH)CO_3$ (Fig. 8) showed two decomposition steps and a weight loss ratio of first and second steps of 1 : 1, expected for the decomposition steps

$$2Sm(OH)CO_3 \xrightarrow{CO_2} Sm_2O_2CO_3 \xrightarrow{CO_2} Sm_2O_3$$

3.3. Effect of carbon dioxide on carbonate decomposition

In order to examine the effect of CO_2-containing gas streams on the thermal decomposition of $La_2(CO_3)_3$, TPD experiments were carried out in mixtures comprising 0, 1, 6 and 17 vol % CO_2 in He (Fig. 9). The presence of CO_2 had minimal effect on the decomposition temperature of $La_2(CO_3)_3$ itself, but the temperature at which $La_2O_2CO_3$ decomposed, shifted to markedly higher temperatures with increasing concentration of CO_2 in the gas stream.

Carbon dioxide is a major product in the oxidative coupling of methane. Thus, both bulk and surface carbonation–decarbonation reactions may well occur under typical oxidative coupling conditions. In case of La_2O_3, the catalyst will then be dominated by dioxocarbonate rather than oxide species at reaction temperatures up to 850 °C. Mechanistic consequences of surface carbonate stability and the presence of bulk dioxocarbonate phases in the working, rare-earth oxide, coupling catalyst are currently being studied.

4. Conclusions

This study has shown that the composition of rare-earth carbonate precipitates varied with both the metal and type of carbonate precipitant. With sodium carbonate, the normal carbonates, $Ln_2(CO_3)_3$, of La, Sm, Tb and Yb were formed. With ammonium bicarbonate as precipitant, only La formed a normal carbonate. With Sm, Tb, Er, and Yb, mixtures of hydroxycarbonates, $Ln(OH)_x(CO_3)_y$ and small amounts of normal carbonates, were obtained. Cerium afforded $CeOCO_3$ irrespective of precipitant.

Rare-earth normal carbonates, $Ln_2(CO_3)_3$, decompose in two distinct steps via the dioxocarbonate, $Ln_2O_2CO_3$, while the hydroxycarbonates, $Ln(OH)_x(CO_3)_y$, and $CeOCO_3$ convert directly to the oxides on heating. The difference in mode of decomposition of $Sm(OH)CO_3$, and $Sm(OH)_x(CO_3)_y$ samples prepared in the present study is attributed to differences in particle size of carbonate precursors.

Gaseous CO_2 has minimal effect on the decomposition of $La_2(CO_3)_3$ to $La_2O_2CO_3$, but the decomposition of $Ln_2O_2CO_3$ to La_2O_3 increases significantly with increasing CO_2 partial pressure.

Acknowledgements

The authors thank Dr D. Hay for XRD, Messrs H. Jaeger for TEM, and J. Newman for TGA analysis. This work was partly supported by a Generic Industry Research and Development Grant, no. 15005 and National Energy Research Development and Demonstration Grant no. 85/0905.

References

1. K. OTSUKA, K. JINNO and A. MORIKAWA, *Catal.* **100** (1986) 353.
2. *Idem, Chem. Lett.* (1985) 499.
3. K. NAGASHIMA, H. WAKITA and A. MOCHIZUKI, *Bull. Chem. Soc. Jpn* **46** (1973) 152.
4. A. N. CHRISTENSEN, *Acta Chem. Scand.* **27** (1973) 2973.
5. H. WAKITA and K. NAGASHIMA, *Bull. Chem. Soc. Jpn* **45** (1972) 2476.
6. R. G. CHARLES, *J. Inorg. Nucl. Chem.* **27** (1965) 1489.
7. R. L. N. SASTRY and S. R. YOGANARASIMHAN, *J. Inorg. Nucl. Chem.* **28** (1966) 1165.
8. J. O. SAWYER, P. O. CARO and L. EYRING, *Rev. Chim. Miner.* **10** (1973) 93.
9. *Idem, L. Spectrochim. Acta* **28A** (1972) 1167.
10. R. P. TURCOTTE, J. O. SAWYER and L. EYRING, *Inorg. Chem.* **18** (1969) 238.
11. J. A. K. TAREEN and T. R. N. KUTTY, *J. Crystal Growth* **50** (1980) 527.
12. O. YAMAGUCHI, K. SUGJURA and K. SHIMIZU, *Z. Anorg. Allgem. Chem.* **544** (1981) 205.
13. M. ALKINC and D. SORDELET, *Adv. Ceram. Mater.* **2** (1987) 232.
14. J. K. MARSH, *J. Chem. Soc* (1941) 561.
15. H. WAKITA, *Bull. Chem. Soc. Jpn* **51** (1978) 2879.

Received 11 June
and accepted 26 June 1990